

# SOLID-PROPELLANT MICRO-THRUSTER

E.A.Parra<sup>1</sup>, K.J.S.Pister<sup>2</sup>, C.Fernandez-Pello<sup>1</sup>

<sup>1</sup>Department of Mechanical Engineering,

<sup>2</sup>Department of Electrical Engineering,

University of California, Berkeley

Berkeley CA 94720-1740

## Abstract

Miniaturization of solid-propellant thrusters is an area of active research that has been motivated by the reduction in size of aerospace systems and the advancement of micromachining techniques. A number of challenges, particularly in the combustion domain, need to be overcome before micro-thrusters with respectable efficiencies can be realized, however. Current designs made primarily out of silicon suffer from high thermal losses and, in extreme cases, flame quenching due to the augmented surface area to volume ratio associated with miniaturization. A millimeter-scale novel composite solid-propellant (AP/HTPB) thruster design that recycles thermal energy and could significantly increase efficiency is here presented. A meso-scale thruster is being tested first to study the operation characteristics of the new design. In addition, propellant formulation has been optimized for the thruster minimization.

*Keywords: thruster, micro-rocket, micro-propulsion, solid-propellant, combustion.*

## 1 - INTRODUCTION

In recent years, there has been a movement towards the miniaturization of devices. This trend can be observed from lab-on-a-chip analyzers to pico-satellites orbiting the earth. The increasing benefit of portability, reduced power consumption, and waste reduction has pushed the research community towards advancements in microfabrication techniques and small-scale theoretical understanding. This interest has also spawned over micro-propulsion. A number of research groups have studied the integration of micro-thrusters for attitude control of micro- and nano-satellites, where controllable burns down to 1 $\mu$ N of thrust are required for maneuvering [1]. Rossi et al. developed a MEMS fabricated solid-propellant micro-thruster (1.5mm) array for this purpose [2]. Bi-propellant centimeter scale thrusters having greater thrust have been developed as shown by Epstein et al [3].

Applications having greater power requirements also exist. These include the deployment system for distributed sensor networks such as Smart-Dust [4] and propulsion for nano-vehicles [1] among others. In these cases, the goal is to maximize the payload capability and the trajectory traveled. Lindsay et al. demonstrated that a millimeter sized silicon chamber utilizing solid-propellant generated 4mN of thrust and could gain elevation under atmospheric conditions [4]. Building on this work that demonstrated flight from a solid propellant micro-thruster, a novel one-time deployment, millimeter scale device is presented. A number of challenges brought by previous designs are addressed with the intent to increase the overall efficiency of the device. These include increasing the residence time of the propellant to allow complete combustion, increasing chamber pressure to reduce combustion loss, addressing the

thermal losses brought by the miniaturization, and modifying the propellant recipe to decrease incomplete combustion.

## 2 - DESIGN METHODOLOGY

Though macro-scale solid-propellant rockets have been thoroughly studied, models that describe these cannot usually describe micro-devices accurately. At the reduced scale, effects like friction become dominant and assumptions such as adiabatic walls become inaccurate. Additionally, combustion becomes more of a challenge due to the reduced device dimensions and the un-scalability of flame sizes and reaction times. To build a successful device, the characteristics that scale well with size must be exploited or a completely new concept devised.

### 2.1 Chamber Geometry

In solid propellant thrusters, the chamber stores the unburned propellant and the combustion reactions once the propellant is ignited. The propellant grain configuration used depends on the application of the thruster, which stretch between  $\Delta v$ , range, or time-to-target [5]. Solid-propellant thrusters are typically cylindrical and have either a core- or an end-burning grain configuration. In the case of micro-thrusters for sensor network deployment, or ranging under atmospheric conditions, it is advantageous to have an end-burning grain for it maximizes the burning time. As it will be shown, increasing the thrust by increasing the mass flow rate through a core burning grain design is not as beneficial. Unfortunately, having an elongated combustion chamber is detrimental to the thermal management of the device furthering the need for a creative geometry.

### Grain Configuration

Neglecting viscous drag, Eq. (1) describes the forces acting on the thruster: propulsion, weight, and pressure drag.

$$\sum F = ma = m v_e - mg - \frac{1}{2} \rho_{air} A_F C_D V^2 \quad (1)$$

Assuming that the thrust is much greater than the weight, as for chemical thrusters, the terminal velocity is achieved quickly, and the distance traveled is approximately linear with burning time. The terminal velocity is found by maximizing Eq. (1) and can be analyzed by substituting in

the steady state mass consumption rate  $\dot{m} = A_b r \rho_{prop}$ , where  $r$  is the burning rate.

$$V_{max} = \sqrt{\frac{2(m v_e - m_f g)}{A_F \rho_{air} C_D}} \cong \sqrt{\frac{2 A_b r \rho_{prop} v_e}{A_F \rho_{air} C_D}} \quad (2)$$

Assuming that  $r$ ,  $v_e$  (gas exit velocity), and propellant density are constant, the follow two cases can be made.

**Core-Burning Grain** - Equation (2) demonstrates that increasing the mass flow rate, which is proportional to the burn area,  $A_b$ , increases the terminal velocity to the half power. On the other hand, this configuration limits the propellant consumption direction to half the diameter, limiting the burning time.

**End-Burning Grain** - Since  $A_b/A_F$  is nearly unity for pressure vessels because of strength requirements (hoop stress), the cross sectional area has little to no effect on the terminal velocity. Additionally, the burning time is maximized for the propellant is consumed along the largest dimension.

### L/D Ratio

As was demonstrated previously,  $V_{max}$  is weakly dependent on cross-sectional area in an end-burning grain. Geometrically, the range is mostly dependent on the thruster length. This means that for a given amount of propellant volume, the distance traveled is linearly proportional to its burning time and loosely related to its diameter. Figure (1) below illustrates this effect. The chamber geometry ( $L/D$ ) is varied while all other parameters are held constant.

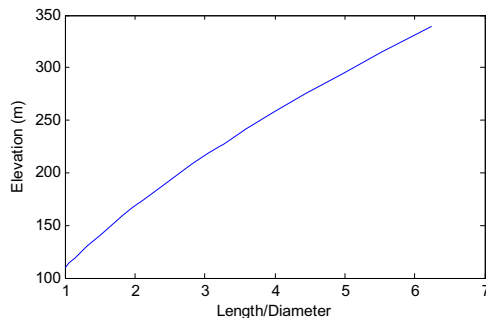


**Figure 1** – Theoretical elevation limit from various  $L/D$  ratios using 130mg of AP/HTPB propellant, assuming  $I_{sp} = 120s$ ,  $C_d = 0.4$ ,  $r = 10mm/s$ ,  $MR=2$ .

Another advantage of elongating the chamber is that the mass ratio ( $MR$ ) increases with  $L/D$ . Since the empty thruster mass consists of a closed cylinder, the propellant mass fraction ( $PMF = m_{prop} / m_o$ ) increases logarithmically with  $L/D$ .

### 2.2 Nozzle

A converging-diverging nozzle that surrounds the chamber is proposed as shown in Fig. (2). This design intends to address the thermal losses associated with a high  $L/D$  end-burning grain thruster. Because the combustion products travel around the chamber through a circulating nozzle, less of a thermal gradient exists at the chamber wall and heat loss is reduced. This is desirable because the combustion temperature is maintained inside the chamber, and the subsonic flow velocity increases with temperature. Likewise, the supersonic flow in the diverging nozzle section is accelerated by the heat loss through the thruster's outer wall. The effects of heat transfer in supersonic nozzle are summarized in Table 1.

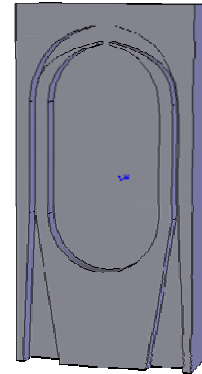


**Figure 2** - Circulating supersonic novel chamber schematic.

**Table 1** - Effect of heat addition on Mach number and velocity[6].

	q	p	M	V
$M < 1$	+	-	+	+
$M > 1$	+	+	-	-
$M < 1$	-	+	-	-
$M > 1$	-	-	+	+

Additionally, because the thruster is more compact, its total weight is reduced, increasing the  $PMF$  and payload capability. A disadvantage of the circulating nozzle is momentum loss incurred by the turn and will be addressed later. Care must be taken to limit the heat transfer from the flow at the exit of the thruster to prevent premature ignition of the unburned propellant inside the chamber. Lastly, the nozzle throat should be designed so that the flow is supersonic but the area is sufficiently large to overcome thick boundary layer effects and expand properly. Studies of viscous effects on cold gas thrusters have been performed and losses have not been found to be significant for flows where the  $Re$  is above 3000 [7]. Below this regime, the flow efficiency decreases significantly, so it will be taken as

the throat diameter lower limiting case. To give a rough estimate, assuming the properties of air at STP, a nozzle throat diameter above 100 $\mu$ m satisfies this condition.

### Specific Impulse

Specific impulse is a metric for propellant efficiency, and it is proportional to the nozzle exit velocity. As it was shown by Eqs. (1-2),  $v_e$  is an important factor in the terminal velocity. For a device with an end-burning grain where the thrust exerted is nearly constant with time, the specific impulse is proportional to the gas velocity at the nozzle exit, as shown below.

$$I_{sp} = \frac{\int F dt}{mg} = \frac{m v_e t}{mg} = \frac{v_e}{g} \quad (3)$$

The nozzle exit gas velocity can be estimated using the isentropic relations through supersonic nozzles [5]. As the size of the thruster is reduced, however, isentropic relations become inaccurate because of increased viscous losses and short chambers which have flows reacting through the nozzle (irreversibilities). Direct numerical simulation (DNS) is needed for accurate modeling and will be performed in future studies. For now, as an approximation, using classical nozzle analysis, the exit velocity is

$$v_e = \sqrt{\frac{2kRT_1}{k-1} \left(1 - \frac{P_{atm}}{P_1}\right)^{\frac{k-1}{k}}} \quad (4)$$

where  $k$  is the specific heat ratio,  $R$  is the universal gas constant and  $P_1$  and  $T_1$  are the pressure and temperature inside the combustion chamber, respectively.

Figure (3) below illustrates the effect of chamber temperature and pressure on gas velocity using Eq. (4). The exit velocity, as can be seen, is a stronger function of temperature than of pressure and increases with both, making the case for mitigating the thermal losses.

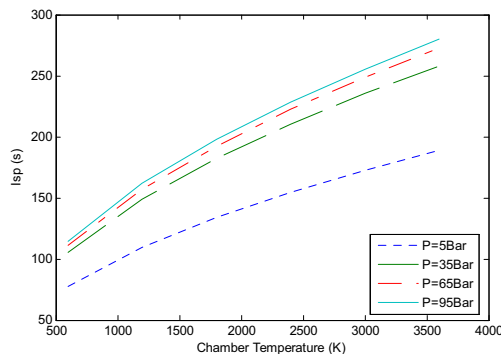


Figure 3 – Isentropic  $I_{sp}$  for various temperatures and pressures.

The maximum chamber temperature for a particular fuel occurs near stoichiometric and at adiabatic conditions. For the dynamic analysis performed earlier, an  $I_{sp}$  of 120s was assumed, which corresponds to pressure of 35atm and a temperature of 700K, a modest performance objective for a micro-thruster. For comparison, the space shuttle solid

rocket boosters use ammonium perchlorate and hydroxyl-terminated polybutadine binder with aluminum particles (AP/HTPB/Al) which has an adiabatic flame temperature around 3200K. At a pressure of 68atm expanded to 1atm, this fuel provides about 256s specific impulse or a nozzle exit velocity of 2.5km/s.

### 2.3 Material

Most micro-thrusters fabricated to date have been out of silicon. This material is ideal for batch fabrication but is not the best suited for combustion chambers. Silicon has a high thermal conductivity and, unless heavily doped, is transparent through the far infrared increasing radiation heat loss. Additionally, silicon is brittle and requires thicker wall dimensions in order to tolerate the pressure spike from ignition. A material with high strength at an elevated temperature that can withstand a corrosive environment should be used. Stainless steel is selected for these reasons. Materials will be reconsidered in the next design cycle to accommodate batch fabrication needs. A fabrication method such as LIGA can be used to create metal chambers of this scale, for example.

### 2.4 Fuel

Solid propellant was chosen to minimize the complexity of the design. Though liquid and bi-propellant fuels have a higher energy density and provide throttle control, these require valves, pressurized storage tanks, and pumps that are not easily incorporated into small devices.

A composite propellant of ammonium perchlorate (oxidizer) and HTPB (polymer binder) is selected for its high energy density. A typical AP/HTPB grain consists of multi-modal oxidizer to reach the 89% Stoichiometric ratio. The oxidizer size modes are generally at coarse and fine diameters of 200 $\mu$ m and 20 $\mu$ m respectively, creating both pre-mixed and diffusion flames [8]. Diffusion flames, however, increase the combustion loss in micro-thrusters. This loss occurs because diffusion-limited reactions require an extended residence time, and the limited dimensions of the thruster maybe unable to house these reactions. Decreasing the oxidizer diameter can aid this problem, however, for it has shown to maximize the premixed flame through better solid mixing. Jeppson et al. has shown that flames are essentially pre-mixed at AP grain sizes smaller than 20 $\mu$ m at 68 atm [8]. In this work, the oxidizer particle size used has been reduced to maximize propellant solid-phase mixing and take advantage of the pre-mixed flame. The effect of oxidizer particle size on micro-thruster performance is studied.

It is common to include metal fuel such as aluminum in the composite propellant because it increases specific impulse. Adding the metal increases the  $I_{sp}$  of macro devices from 200 to about 250 seconds for this composite propellant at sea level [9]. The addition of aluminum, however, is not recommended in small devices for the following reasons.

Because aluminum combusts in the gas-phase at very high temperatures, the lower chamber temperatures typical of small thrusters are not sufficient to oxidize the metal. Consequently, the aluminum agglomerates at the burning surface and detaches as large liquid drops of up to 300  $\mu\text{m}$  in diameter [10]. The liquid agglomerates do not follow the streamlines and cause momentum loss of the gas due to two-phase flow. It also absorbs energy from the gaseous higher temperature products. Additionally, the liquid metal clogs the nozzles which are typically in the 100's of  $\mu\text{m}$  scale. Lastly, the metal that successfully converts into solid alumina erodes the nozzle altering its dimensions.

### 3 - EXPERIMENT

A number of thruster designs are being studied. Figure (4) illustrates a circulating and a baseline rectangular nozzle design. The circulating supersonic nozzle previously presented is also being tested. Rectangular nozzles are included because these produced greater thrust in previous studies. Combustion chambers are 12mm in length and 6mm in diameter. The nozzle throats are 0.35mm in width. The instantaneous thrust is measured through a pendulum apparatus, shown in Fig. (5), and the thrust force is sensed through a piezoelectric transducer.

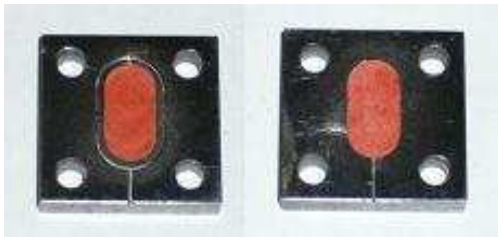


**Figure 4** – Circulating rectangular nozzle and baseline short nozzle before testing.

A number of variables are being experimentally tested. Specifically, the effects of recycling thermal energy, increasing the residence time, and enhancing solid phase mixing are studied.

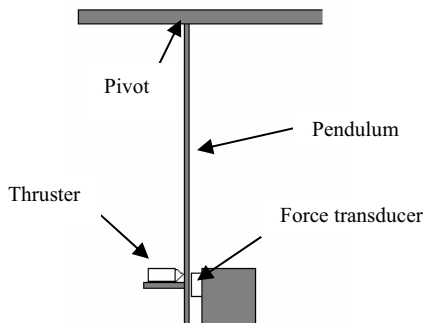


**Figure 5** - Schematic of thrust measuring apparatus.

Combustion is initiated through a glow plug, a resistive heater commonly used in RC gas engines. The thrust of each of the designs is tested with propellants using

unimodal oxidizer particles of nominal sizes of 20 $\mu\text{m}$ , 90 $\mu\text{m}$ , and 250 $\mu\text{m}$ . The chambers are filled with 130mg of AP/HTPB propellant at 85% oxidizer loading.

### 3 - PRELIMINARY RESULTS

Preliminary results indicate that propellant is deflagrating fully. Increasing the chamber pressure has reduced solids inside of the chamber after ignition. Thrust peaks of up to 2.4N have been measured using 200 $\mu\text{m}$  AP.

### REFERENCE

- [1] Micci, M., Ketsdever, A., Micropropulsion for Small Aircraft, Progress in Astronautics and Aeronautics, Vol. 187, 2000.
- [2] Rossi, C. et al “A New Generation of MEMS Based Microthrusters for Microspacecraft Applications”, Proc. MicroNanotechnology for Space Applications, Vol. 1, April 1999.
- [3] A.H. Epstein, S.D.Senturia, O.Al-Midani, G.Anathasauresh and al, .Micro-Heat Engines, Gas Turbines, and Rocket Engines - The MIT microengine Project., AIAA, 1997.
- [4] Lindsay, L., Teasdale, D., Milanovic, V., Pister, K., Pello, C., 2001, “Thrust and Electrical Power from Solid Propellant Microrockets”, Proc. 1Jth Annual Int. Conf. on Microelectromechanical Systems (MEMS 2001), Interlaken, Switzerland, 2001, 606-610.
- [5] Sutton, G.P. Rocket Propulsion Elements, John Wiley & Sons, Inc., 2001
- [6] Oosthuizen, P., Compressible Fluid Flow, McGraw-Hill, pp. 278, 1997.
- [7] S.P. Grisnik, T.A. Smith, L.E. Salz, ‘Experimental Study of Low Reynolds Number Nozzles’, AIAA Paper 870092, May 1987.
- [8] M. B. Jeppson, M. W. Beckstead, and Q. Jing, “A Kinetic Model for the premixed Combustion of Fine AP/HTPB Composite Propellant”, AIAA-1998-447 Aerospace Sciences Meeting and Exhibit, 36th, Reno, NV, Jan. 12-15, 1998
- [9] dutlisa.lr.tudelft.nl/Propulsion/Data/Solid\_propellant\_data.ht
- [10] Summerfield, M., Solid Propellant Rocket Research, pp. 253-287, 1960.